REVERSE BIAS VOLTAGE TESTING OF 8 CM X 8 CM SILICON SOLAR CELLS

T. Woike, S. Stotlar, C. Lungu
Applied Solar Energy Corporation
City of Industry, CA

ABSTRACT

This paper describes a study of the reverse I-V characteristics of the largest space-qualified silicon solar cells currently available (8 cm x 8 cm) and of reverse bias voltage (RBV) testing performed on these cells. This study includes production grade cells, both with and without cover glass. These cells span the typical output range seen in production. Initial characteristics of these cells are measured at both 28°C and 60°C. These measurements show weak correlation between cell output and reverse characteristics. Analysis is presented to determine the proper conditions for reverse bias voltage stress to simulate shadowing effects on a particular array design. After performing the reverse bias voltage stress the characteristics of the stressed cells are remeasured. The degradation in cell performance is highly variable which exacerbates cell mismatching over time. The effect of this degradation on array lifetime is also discussed. Generalization of these results to other array configurations is also presented.

I. INTRODUCTION

The use of large area solar cells in solar arrays for space applications has become more pervasive as the fabrication technology and the cost-effectiveness of these cells improve. These large cells are more defect prone than smaller cells of equivalent defect density. This results in an adverse effect on the reverse current - voltage (I-V) characteristics of the cells. These characteristics become important during periods of partial shadowing in solar arrays that do not incorporate shunting or bypass diodes. The impact of the quality of cell reverse I-V characteristics on the cell lifetime is manifested as the well-known "hot spot" effect (Blake,1969). Reverse bias voltage stress testing is a standard technique that is used to simulate the effects of shadowing when investigating cell lifetime under shadowed conditions (Rauschenbach, 1972).

The objectives of this study were to determine the relationship between cell output and reverse I-V characteristics, if any, and to examine the effects of shadowing on cell forward and reverse I-V characteristics when installed into a particular array configuration without the benefit of bypass diodes.

A number of silicon 8 cm x 8 cm solar cells were obtained from the production line. These were Class I Electrical cells. One-fourth of these cells had cover glass applied, and the remainder were unglassed. The AM0 output data of these cells were measured in production. The reverse characteristics of these cells were later measured at both 28°C and 60°C. These data sets are discussed in Section II.

An analysis was performed to establish the bias conditions that would be produced on a shadowed cell in the array. This analysis required the use of the physical and electrical layout of the array design, the forward and reverse I-V data of the cells, and some assumptions about the size, location, and duration of shadows. The shadowing analysis is presented in Section III.

Reverse bias voltage (RBV) stress testing was then performed on a number of cells. The cells that were used in this phase of the study were chosen to provide a distribution of initial output levels and reverse characteristics. Prior to RBV the cells chosen for the sample were measured for output at 10mW/cm^2 (2800°K source). Each cell was then stressed at a reverse bias voltage that was based on the cell's individual reverse characteristics. This relationship was determined from the shadowing analysis. Various stress durations from a minimum of 2 minutes to a maximum

of 48 hours were used. After RBV stress testing, the output was remeasured at 10 mW/cm^2 and the resulting degradation analyzed. The results of the RBV stress testing are discussed in Section IV.

II. INITIAL CELL CHARACTERISTICS

Cell Distribution among Output Groups

132 silicon 8 cm x 8 cm solar cells were obtained from production. These were Class I Electrical cells. One-fourth of these cells had cover glass applied, and the remainder were unglassed. The AM0 output data of these cells were measured in production. The distribution of cells among the output groups is shown in Figure 1. The definition of these groups is provided in Table 1.

Initial Reverse I-V Characteristics

The reverse characteristics of these cells were measured at both 28°C and 60°C. The results are given in Figures 2 and 3, respectively. Each figure shows the I-V data for the best and worst cells, along with the median cell. This information is presented for both glassed and unglassed cells. Near ambient temperature (Figure 2), the glassed cells exhibit significantly more leakage than their unglassed counterparts. The worst glassed cell is about a factor of four leakier than the worst unglassed cell, the median glassed cell is roughly a factor of three leakier than the median unglassed cell, and the best glassed cell is nearly two orders of magnitude leakier than the best unglassed cell. At slightly elevated temperature (Figure 3), the glassed and unglassed leakage characteristics become nearly indistinguishable, with a typical glassed cell only 25% leakier than an unglassed one. In fact, the leakage of all three benchmark cells (best, worst, median) actually decreases as the cell temperature is increased from 28°C to 60°C. This behavior may be due to residual contamination from the clean performed on the cells prior to glassing. The 60°C leakage current data is more germane to operation in a solar array, provided that power dissipation of a reverse-biased cell is small, as defined in the next paragraph.

Neglecting the effects of power dissipated in the array interconnect and the cell metallization, the temperature of a cell will remain the same when it is shadowed if the additional power dissipation from the reverse-biased condition exactly balances the loss of power absorbed from illumination. If the front-facing absorptance is 0.4, then 3.46 W may be dissipated by a shadowed cell without affecting cell temperature, assuming only radiative heat loss.

Relationship of Initial Cell Reverse Characteristics to Initial Output

The relationship of cell reverse electrical characteristics at 60°C to the output is shown in Figures 4 and 5 with both glassed and unglassed cells identified separately. Figure 4 shows the dark reverse leakage current I_{dr} for all the cells included in this study as a function of cell group number. I_{dr} was measured at 1 V. Figure 5 depicts the reverse breakdown V_{br} as a function of cell group number at a dark reverse current of 1 A. All measurements were taken instantaneously so that the cell would not have time to heat.

There seems to be a rather weak correlation between reverse characteristics and output. The higher group cells generally have better reverse characteristics: lower leakage current and higher breakdown voltage. This is expected since the defects that contribute to the leakage current (bulk and surface defects) will also cause a lower minority carrier lifetime, resulting in lower cell output. Although this general trend is observed in the data, there is a great deal of variability in the data ($r^2 < 0.2$), so there are also other significant factors involved (for example, perimeter defects).

III. SHADOWING ANALYSIS

A worst-case analysis was performed to establish the bias conditions that would be produced on a shadowed cell in the array. This analysis was performed for an array that uses series strings of 120 cells. The following assumptions were made about the solar array and various conditions which affect it. All cells in the array are assumed to have identical electrical characteristics. All series strings of solar cells are assumed to be connected directly to the bus, so that all strings have the same voltage. Resistive losses in the cell and array interconnect are assumed negligible.

A shadow is assumed to not affect the array voltage. The cells in fully illuminated strings are assumed to be biased at the maximum power level. The shadow is assumed to cover the area of a single cell only, since this results in the worst-case reverse bias across the shadowed cell (Blake, 1969). The shadow is assumed to persist long enough to allow the shadowed cell to reach steady-state temperature.

Figure 6 shows the 28°C and 60°C output characteristics that were used for the cells. The cell output parameters are also tabulated in Figure 6. Based on the above assumptions, if the array is operating at 60°C, each illuminated cell will supply 0.438 V, leading to a voltage V_a = 52.6 V across a fully-illuminated string of 120 cells in series. This voltage will also appear across a partially-shadowed string according to the assumptions. This information along with the reverse characteristics of a shadowed cell can be used to determine the voltage and current levels in the shadowed string (Rauschenbach, 1972) as demonstrated in Figure 7. The bias point is determined by the intersection of the characteristics of the 119 illuminated cells with the reverse characteristics of the shadowed cell offset by V_a. The cell reverse characteristics at 60°C (Figure 3) are represented by the relation $I = CV^{1.02}$ where C is the leakage current measured at -1 V.

The bias point for the single shadowed cell was determined for various array configurations as a function of cell leakage current at -1 V using the above technique. The results of this analysis are presented in Figure 8.

IV. REVERSE BIAS VOLTAGE (RBV) STRESS TESTING DISCUSSION AND RESULTS

Reverse bias voltage (RBV) stress testing was performed on a number of cells. The cells that were used in this phase of the study were chosen to provide a good representation of initial output levels and reverse characteristics. Prior to RBV the cells chosen for the RBV sample were measured for output at 10mW/cm^2 (2800°K source). This source was chosen because of better availability than the AM0 simulator. The relation of Figure 8 was used to determine the appropriate stress voltage for each cell.

Short-term RBV Stress

Six cells, four glassed and two unglassed, were subjected to RBV for a series of short duration stresses. Two of these cells underwent a series of three stresses, another two underwent two stresses, and the final two underwent only one stress. The durations of these stresses were such that the total stress times on the cells at the readpoints were 2 minutes, 10 minutes and 40 minutes. After each RBV stress, the output was remeasured at 10 mW/cm^2. The results of the changes in I_{sc}, V_{oc}, and power output are given in Figures 9 through 11, respectively. The changes in I_{sc} dominate the changes in power output of the cells. V_{oc} changes relatively little. At the end of 40 minutes of total stress, all six cells had degraded in power output, with the changes ranging from 2% to 16%. Some cells apparently exhibited stages of healing, perhaps through some sort of self-annealing, but the level of improvement never exceeded the measurement reproducibility.

Long-term RBV Stress

Thirteen different cells were subjected to long-term RBV stress, seven for two hours and the other six for 48 hours. This study was performed to extend the stress duration significantly beyond the usual level (Williams, 1984) and develop a lifetime model for shadowed cells. The post-stress characteristics appear in Figures 12 through 16. The short-term RBV results discussed above have been included in these figures for completeness. As before the output changes are determined mostly by I_{sc} changes, with V_{oc} changes being relatively minor. The unglassed cells show a definite trend toward long-term degradation, as do the glassed cells with the notable exception of three cells that underwent the 48 hour RBV stress and improved slightly from their pre-stress output levels.

Six of the 19 cells studied had their output power degrade by more than 25%, half after 2 hours total stress and the other half after 48 hours stress. Half of these cells were glassed and half were unglassed.

These same six cells also had their reverse breakdown voltage degrade by more than 50%. Three cells (all unglassed) had their reverse leakage current degrade by greater than a factor of ten. The leakage current of the

glassed cells probably did not degrade as rapidly because they have a significant strain-induced leakage component which is not affected by RBV stress aging.

Relationship of Output Degradation to Initial Output

The relationship between cell output degradation and the initial output is demonstrated in Figure 17. It does appear more likely for a higher output cell to undergo more rapid output degradation. This effect has been previously observed (Rauschenbach, 1972) and may be attributed to the higher voltage at which these cells are stressed per Figure 8.

Relationship of Output Degradation to Initial Leakage

The relationship between cell output degradation and the initial leakage was examined since a potential relation between the initial cell output and the leakage had been noted. The power degradation is plotted against the initial cell leakage in Figure 18. The power degradation exhibits a moderate relationship to the initial leakage current level, with the lower leakage cells having more rapid output degradation. This result provides additional validation for the behavior presented in the previous section.

Relationship of Change of Reverse Characteristics to Initial Output

The relationship between the change of cell reverse characteristics and the initial cell output level was also examined because it could help corroborate the results of the previous sections. The results as shown in Figure 19 indicate that the cells having lower output do not degrade as quickly as the better cells.

Relationship of Output Degradation to Change of Reverse Characteristics

Having noted that the poorer cells both in the forward and reverse directions fare better during RBV stress testing, the change in reverse cell characteristics due to RBV was examined to see if this could be used as a predictor of output degradation. The results are presented in Figure 20. A moderate correlation does exist between the change in power output and the change in reverse leakage current, with an increase in leakage indicating a decrease in power output. However these data have a sufficient amount of scatter to preclude any hope of using change in I_{dr} as the only measure of cell degradation without having to perform the output test.

Predicted Lifetime of Shadowed Cell

A simple model for the lifetime of a shadowed cell was developed from a regression performed on the output power degradation data. The results are shown in Figure 21. Selected values from this data set are given in Table 2. Unglassed cells will reach half power with a mean time to occurrence of 116 hours (0.7 weeks) of shadow while the equivalent value for glassed ones is 497 hours (3.0 weeks) of shadow. When the variability of the data is considered, the earliest time (-3σ) to degrade to the half power level is 15.7 minutes of shadow for glassed cells and 44.6 minutes of shadow for unglassed cells. This model can aid in the prediction of array lifetime when combined with shadowing patterns, end-of-life power requirements and other system-level information.

V. CONCLUSIONS

A study of the behavior of 8 cm x 8 cm silicon solar cells under worst-case shadowing conditions was performed for a particular solar array without the benefit of bypass diodes. This study involved analyzing the bias conditions expected to be generated by shadowing and the subsequent RBV stressing of production grade solar cells consistent with the shadowing analysis.

Approximately 32% of the cells that underwent RBV stress testing degraded significantly. This strongly indicates the reliability benefits of incorporating bypass diodes into the design of space-based solar arrays.

With some exceptions, RBV stress testing degraded solar cell output between 2% and 59%. The level of degradation is highly variable and indicates that an initially perfectly matched string of solar cells will become unmatched over time. Furthermore, this variability may be understated since the harsh space environment could not be fully reproduced in this study. A few cases of increases in output after RBV stress testing were observed, but even these may be considered undesirable because this further disturbs the cell matching characteristics of the array.

Glassed cells were predicted to degrade to half power with a mean time to occurrence of 497 hours of shadow while unglassed cells will do so after 116 hours. Initial (-3σ) occurrences are predicted after 15.7 and 44.6 minutes of shadow for glassed and unglassed cells, respectively.

There is a rather weak relationship between the initial reverse characteristics of a cell and that cell's initial output, with the higher output level cells having better reverse characteristics. This correlation is too weak to permit a prediction of cell output performance from its reverse characteristics.

Cell output is inversely related to degradation level from RBV stress testing. Cells having higher output degraded more rapidly than lower output cells. Also cell output and reverse characteristics appear to be correlated both in initial values and change levels. Cells having poorer reverse characteristics did not degrade as rapidly as better cells. These results may be due to the lower voltage levels at which the poorer cells are stressed.

Reverse voltage on a shadowed cell is greatly dependent on the cell's reverse characteristics in high voltage arrays, but in low voltage arrays the reverse voltage is nearly independent of cell reverse characteristics. The highest stress voltage is generated on low leakage cells in high voltage arrays.

The correlation between reverse change and output change was not observed to be strong enough to obviate the need for a cell output test when evaluating cell degradation.

Shadowing on a solar array which does not utilize bypass diodes is predicted to create a permanent output mismatch in a string of cells and exacerbate this mismatch over time. This effect is accelerated in high-voltage arrays since the bias levels on shadowed cells are higher. This undesirable and somewhat unpredictable effect can be avoided by incorporating bypass diodes into the design of solar arrays.

REFERENCES

Blake, F.A., and K.L. Hanson. 1969. The "Hot-spot" Failure Mode for Solar Array. Proceedings of the IECEC. pp. 575-581.

Rauschenbach, H.S., and E.E. Maiden. 1972. Breakdown Phenomena in Reverse Biased Silicon Solar Cells. Proceedings of the Ninth IEEE Photovoltaic Specialists Conference. pp. 217-225.

Williams, R.D., G.S. Goodelle, and N. Mardesich. 1984. Solar Cell Reverse Bias Testing to meet New Cell Technology and Satellite Applications Demands. Proceedings of the Seventeenth IEEE Photovoltaic Specialists Conference. pp. 306-309.

TABLE 1

Solar Cell Output Groups

Output Current
I_L Measured @ 0.495 V; 28°C

Group	Minimum I_L (mA)	Maximum I_L (mA)
1	2217	2253.9
2	2254	2290.9
3	2291	2327.9
4	2328	2364.9
5	2365	2401.9
6	2402	2438.9
7	2439	2475.9
8	2476	2512.9
9	2513	2549.9
10	2550	None

TABLE 2

Predicted Total Shadow Time to Degrade
Shadowed Cells to Specified Power Level

(120 cells in a string)

	Glassed		Unglassed	
Normalized Power	Earliest Predicted Occurrence	Mean Time to Occurrence	Earliest Predicted Occurrence	Mean Time to Occurrence
1.00	0.0 hr	0.0 hr	0.0 hr	0.0 hr
0.75	0.1 min	4.3 hr	1.5 min	3.9 hr
0.50	15.7 min	497.4 hr	44.6 min	116.1 hr
0.25	30.6 hr	6.6 yr	22.0 hr	0.4 yr

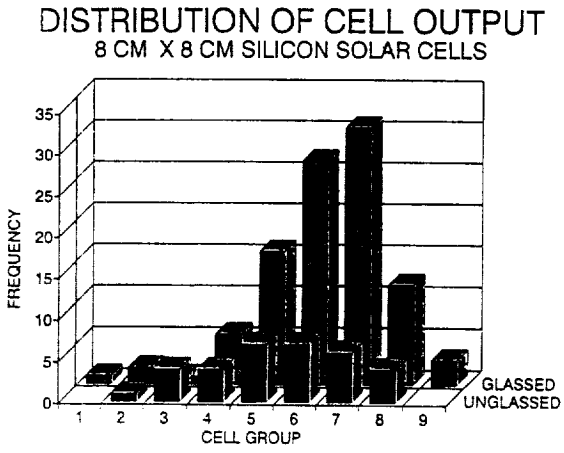

FIGURE 1

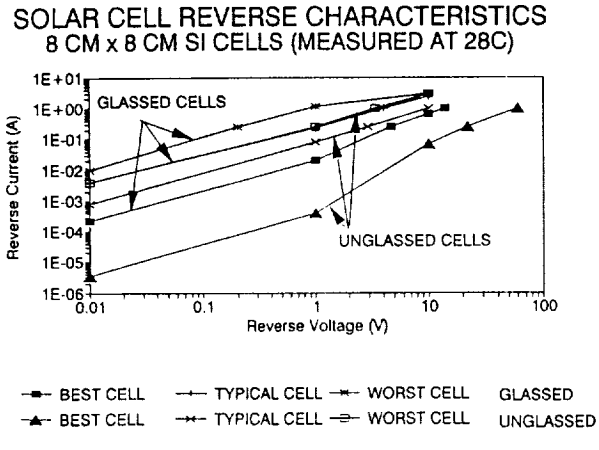

FIGURE 2

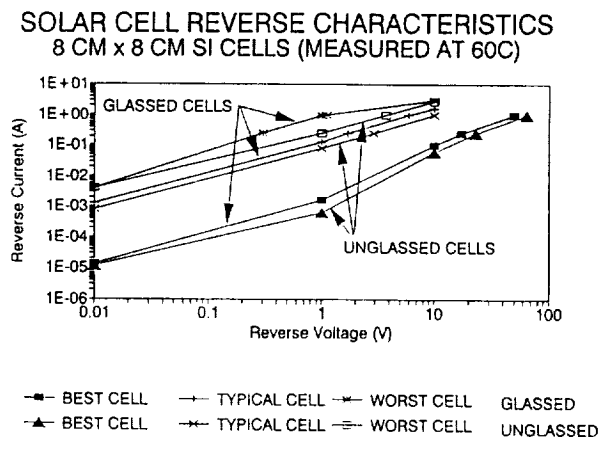

FIGURE 3

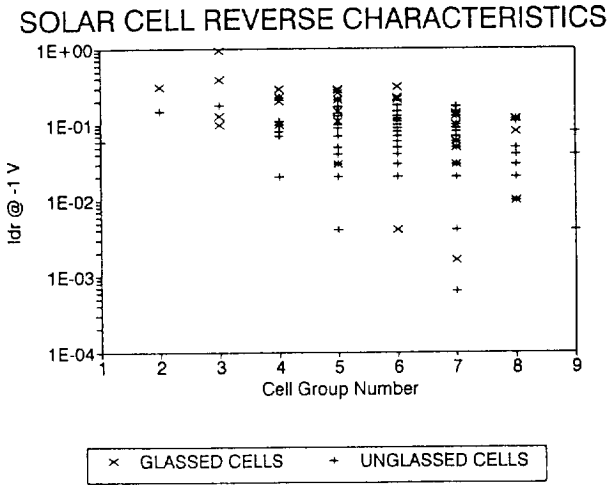

FIGURE 4

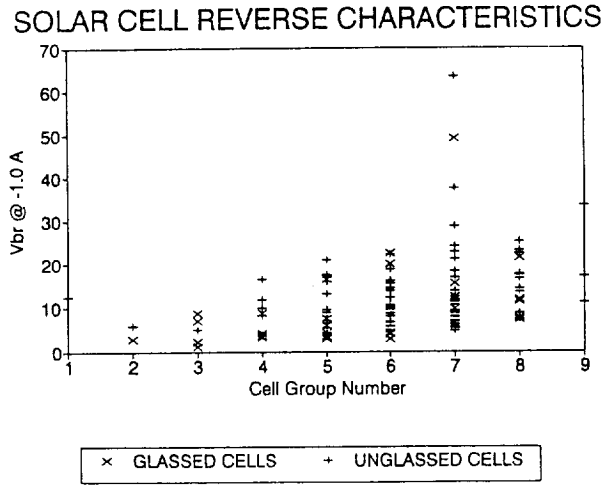

FIGURE 5

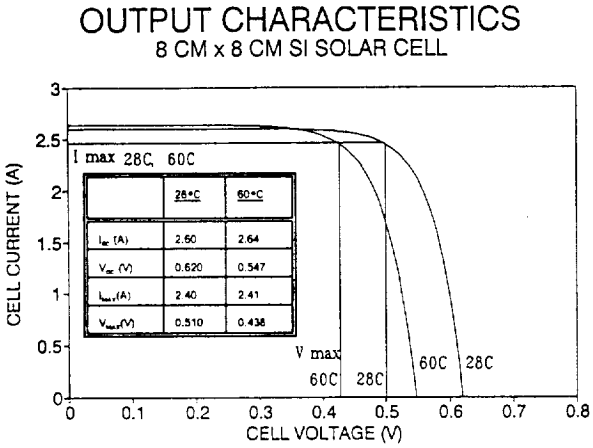

FIGURE 6

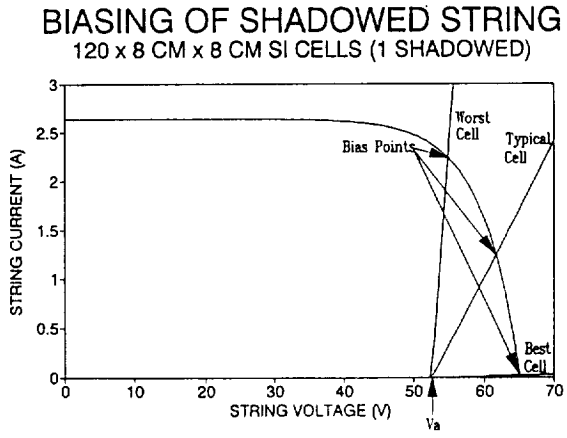

FIGURE 7

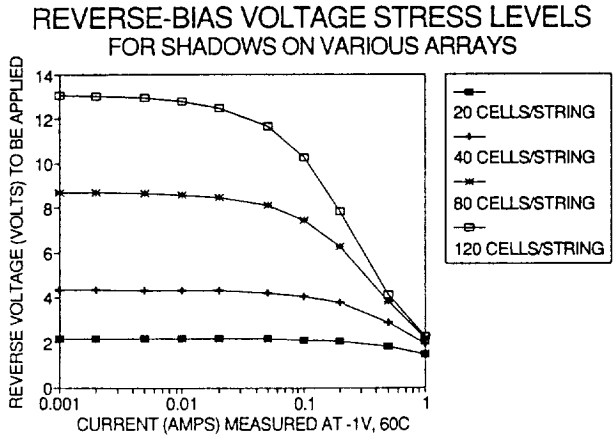

FIGURE 8

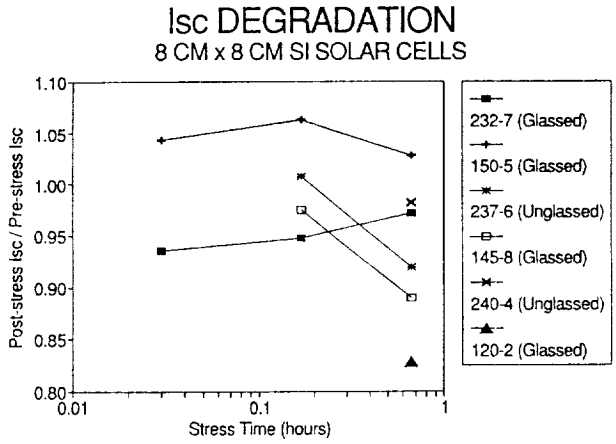

FIGURE 9

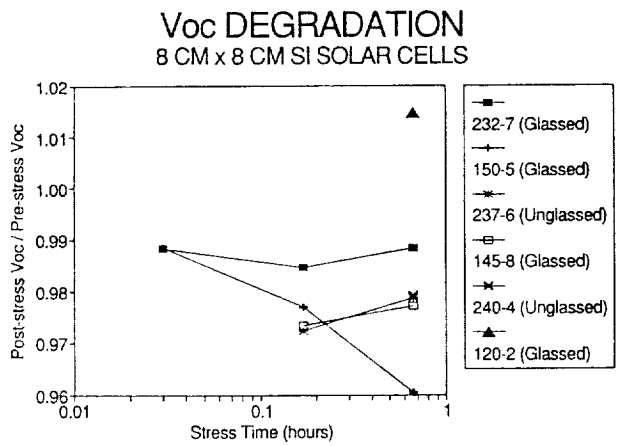

FIGURE 10

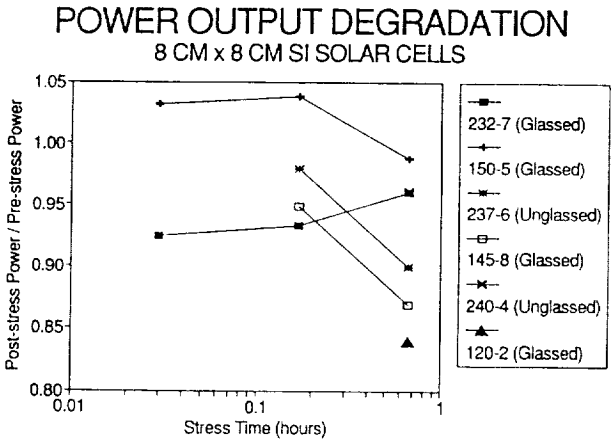

FIGURE 11

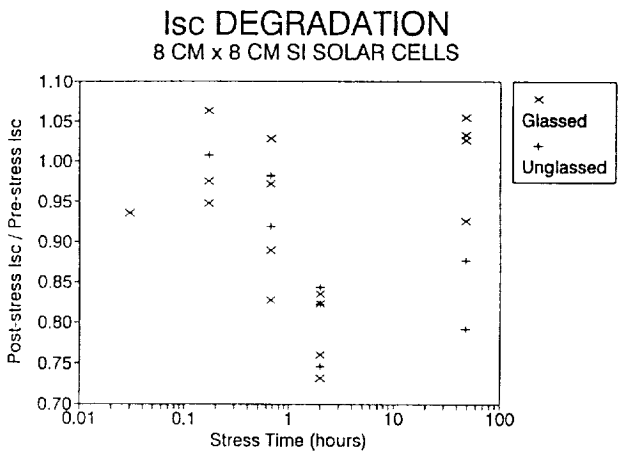

FIGURE 12

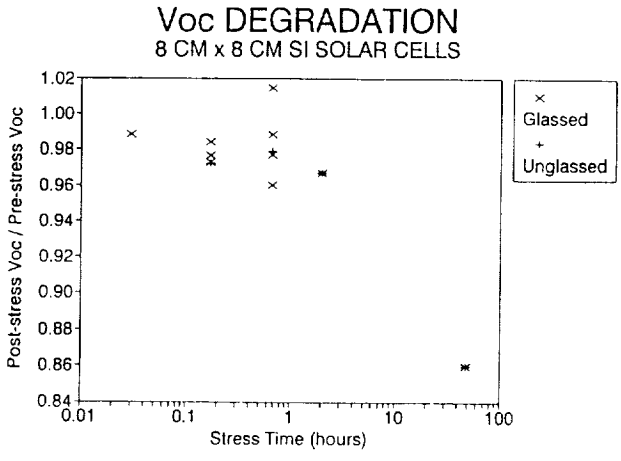

FIGURE 13

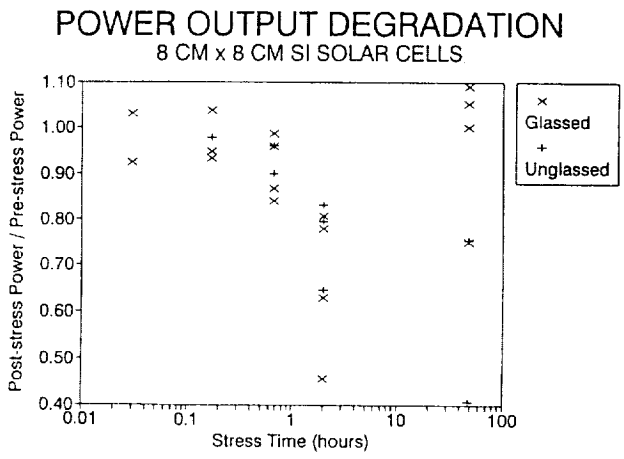

FIGURE 14

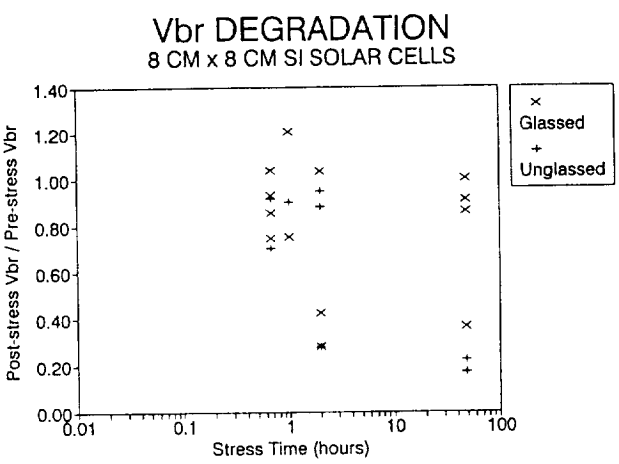

FIGURE 15

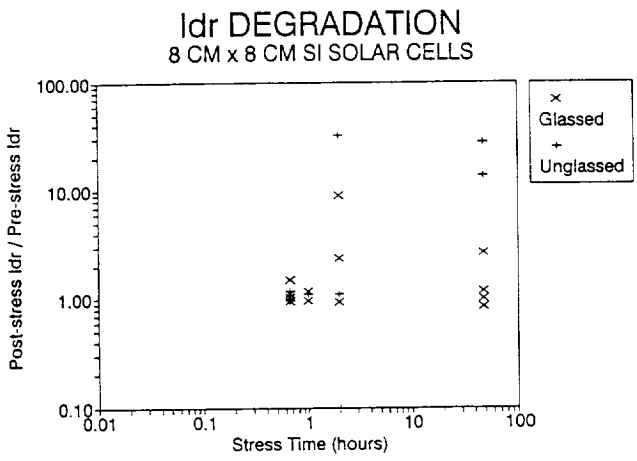

FIGURE 16

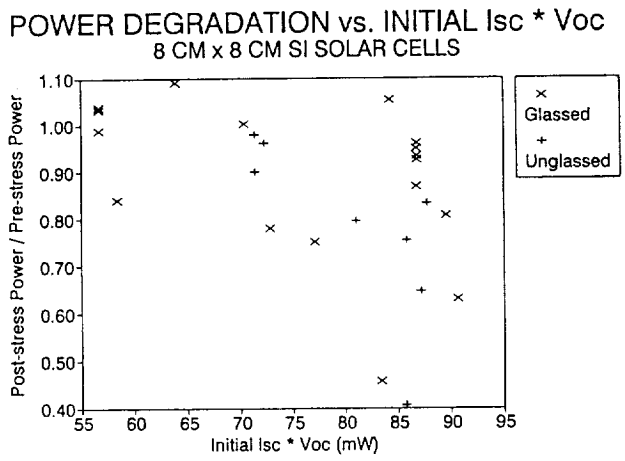

FIGURE 17

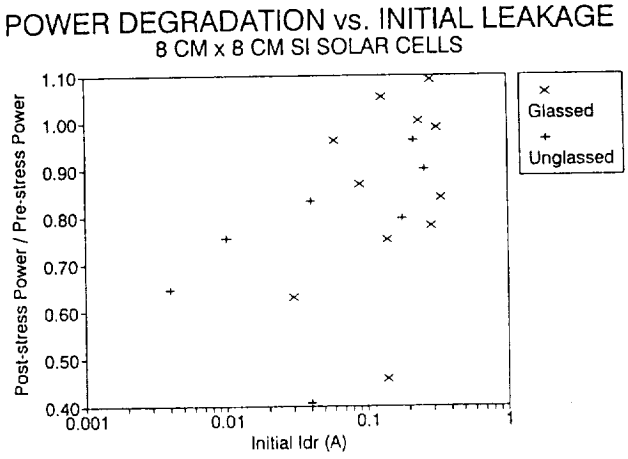

FIGURE 18

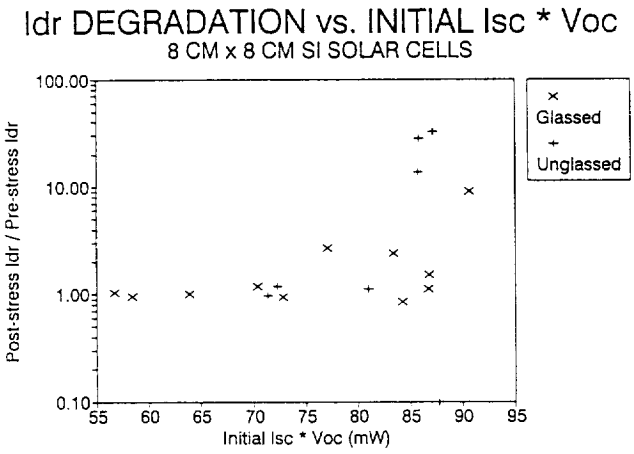

FIGURE 19

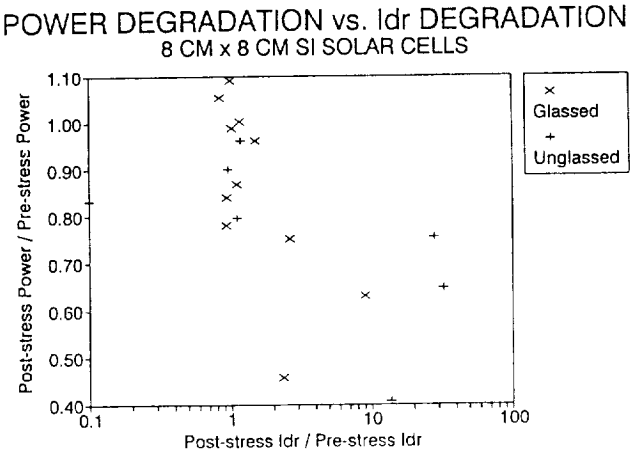

FIGURE 20

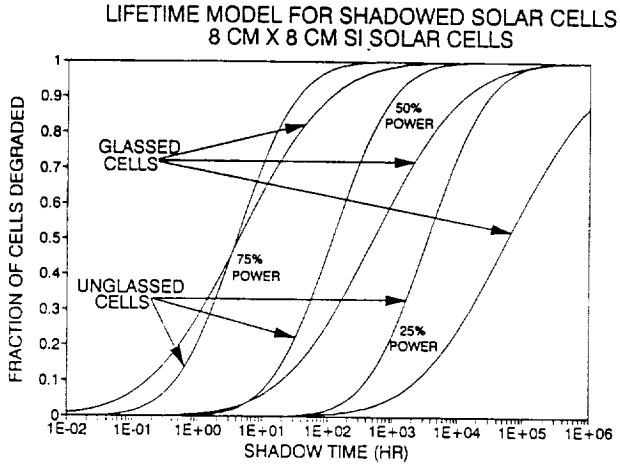
LIFETIME MODEL FOR SHADOWED SOLAR CELLS
8 CM X 8 CM SI SOLAR CELLS
FRACTION OF CELLS DEGRADED
SHADOW TIME (HR)
GLASSED CELLS
UNGLASSED CELLS
50% POWER
75% POWER
25% POWER
1
0.9
0.8
0.7
0.6
0.5
0.4
0.3
0.2
0.1
0
1E-02
1E-01
1E+00
1E+01
1E+02
1E+03
1E+04
1E+05
1E+06

FIGURE 21